Central nucleus-nucleus collisions at relativistic energies with a new method based on Random Matrix Theory

Z. Wazir[1;1)] R. G. Nazmitdinov[2,3] E. I. Shahaliev[4,5] M. K. Suleymanov[1,4]

[1] Department of Physics, COMSATS Institute of Information Technology, Islamabad, Pakistan
[2] Department de Fisica, Universitat de les Illes Balears, E-07122 Palma de Mallorca, Spain
[3] Bogoliubov Laboratory of Theoretical Physics, Joint Institute for Nuclear Research, 141980 Dubna, Russia
[4] High Energy Physics Laboratory, Joint Institute for Nuclear Research, 141980, Dubna, Russia
[5] Institute of Radiation Problems, 370143, Baku, Azerbaijan

Abstract Using the method based on Random Matrix Theory (RMT), the results for the nearest-neighbor distributions obtained from the experimental data on ^{12}C-C collisions at 4.2 AGeV/c have been discussed and compared with the simulated data on ^{12}C-C collisions at 4.2 AGeV/c produced with the aid of the Dubna Cascade Model. The results show that the correlation of secondary particles decreases with an increasing number of charged particles $N_{\rm ch}$. These observed changes in the nearest-neighbor distributions of charged particles could be associated with the centrality variation of the collisions.

Key words random matrix theory, experimental data, Dubna cascade model, central collisions

PACS 25.75.Gz, 25.75.Dw, 25.75.Nq

1 Introduction

Centrality of collisions [1–6] depends upon various characteristics of particle production at nuclear-nuclear collisions. In various experiments the centrality is defined as a number of identified protons, projectile and target fragments, slow particles, all particles, even as the energy flow of the particles with emission angles equal to 0° or 90°, etc. These methods enable one to establish approximately the centrality using the number of secondary charged particles in experimental data and, in particular, from the number of secondary charged particles simulated with the aid of the Dubua Cascade Model. Evidently, the absence of an unambiguous criterion for the centrality may significantly affect the interpretation of model results and, therefore, hide a true signal on the onset of a new phase of the hadronic matter. In this paper [7] we suggest that tools from RMT [8, 9] might be useful in illuminating the presence of correlations in the spectral (momentum) distribution of secondary particles produced in nucleus-nucleus collisions at high energy. In fact, we have found good agreement between the results obtained with the aid of the RMT approach and a standard analysis based on the method of effective mass spectra and two-pair correlation function often used in high energy physics [10]. The RMT approach does not depend on the background of measurements and relies only on fundamental symmetries preserved in nucleus-nucleus collisions. The purpose of the present paper is to demonstrate the decrease in correlation with an increase in the number of charged particles $N_{\rm ch}$ and to suggest a criterion to the centrality of collision, using a method based on the RMT approach.

2 Experimental data

We use the experimental data which were obtained from the 2-m propane bubble chamber of the Laboratory of High Energy, JINR [11–13]. The 2 m propane bubble chamber, placed in a magnetic field of 1.5 T, was exposed to the beams of nuclei at the Dubna synchrophasotron. All secondary particles, emitted at a 4π total solid angle, were detected in the chamber. All negative particles, except for

Received 20 November 2009

1) Corresponding author: zafar_wazir@yahoo.com

those identified as electrons, were considered as π^--mesons. The contamination from the misidentified electrons and the negative strange particles did not exceed 5% and 1%, respectively. The minimum momentum for pion registration is about 70 MeV/c in the lab frame (we consider all kinematic variables in the lab frame). The protons were selected by a statistical method applied to all positive particles with a momentum of $|p|>500$ MeV/c (slow protons with $|p|\leqslant 700$ MeV/c were identified by ionization in the chamber). The maximum particle production was observed at $|p|\approx 0.5$–0.7 GeV/c. The particle momenta were calculated from the particle trajectories in a magnetic field, taking into account the ionization and radiation losses. In particular, the uncertainties in the momentum value were estimated, taking account of the effects of multiple Coulomb scattering and bremsstrahlung radiation. The average uncertainty in the momentum and the angle measurements varies as $\langle \Delta p/p\rangle = (11.5\pm 0.3)\%, \langle \Delta\theta\rangle \approx 0.8^\circ$. In this experiment, there were 37792 ^{12}CC interaction events at a momentum of 4.2 AGeV/c [12–14].

3 Dubna Cascade Model

The Dubna Cascade Model (DCM) [15–20] is an example of a microscopic model, which follows the concept of the intranuclear cascade. In the intranuclear cascade models, only the nucleon-nucleon collisions are described. The mean field is taken to be a constant. Therefore, the particles propagate along straight trajectories until they collide with each other or with the potential wall. The cascade of sequential interactions is tracked in time by the Monte-Carlo technique. The nucleon-nucleon collision scheme of the interaction corresponds to a short-range hard-core potential. In the simplest approach it is assumed [15–20] that, due to the interaction of a projectile hadron with one of the target nucleons, the creation of a new particle takes place. The participating target nucleon accepts momentum and begins to move in the nucleus. All moving (cascade) particles can interact with other nuclear nucleons to produce new particles or suffer elastic rescattering. Therefore, cascade reproduction of moving particles is assumed. The interactions between cascade particles are omitted as a rule. The process continues until all moving particles either leave the nucleus or are absorbed. Due to the analysis of fast particles and correlations between slow and fast particles the DCM [21] was recognized as one of the best models applied to intermediate energy physics [22]. In the initialization phase, the DCM takes into account the diffuseness of the nuclear potential well. The model is formulated in a relativistic framework. π-meson and Δ-resonance production are included. At an advanced stage of the interaction, particles can be emitted from both equilibrium and non-equilibrium states.

We used the simulated data that have been obtained from the DCM [23]. We have generated 200000 events of ^{12}C-C collisions at 4.2 AGeV/c in the lab frame.

4 Methodology

Our method is based on the RMT [7–10], which was originally introduced to explain the statistical fluctuations of neutron resonances in compound nuclei [24]. The theory assumes that the Hamiltonian belongs to an ensemble of random matrices that are consistent with the fundamental symmetries of the system. Since the nuclear collisions preserve time-reversal symmetries, the relevant ensemble is the Gaussian Orthogonal Ensemble (GOE). When the time-reversal symmetry is broken, one can apply the Gaussian Unitary Ensemble (GUE). The GOE and GUE correspond to ensembles of real symmetric matrices and of Hermitian matrices, respectively. Besides these general symmetry considerations, there is no need in other properties of the system under consideration. Based on this method, we consider the ordered sequence of energy levels $\{E_i\},\ i=1,\cdots,N$ (momentum distribution) to have an average density of states $\rho_{\rm av}\ (E)$. From this sequence, a new one is obtained by the unfolding procedure of the original spectrum $\{E_i\}$ through the mapping $E\to x$

$$x_i=\int_0^{E_i}\rho_{\rm av}(E'){\rm d}E'=\int_0^{x_i}{\rm d}x'=\zeta(E_i),\ i=1,\cdots,N, \tag{1}$$

where, $\zeta(E_i)$ is the smoothed function giving the number of eigenvalues less than or equal to E_i of the exact eigenvalue distribution $N(E_i)$ (see details in Ref [10]). The effect of mapping is that the sequence $\{x_i\}$ has, on average, a constant mean spacing equal to one (or a constant density), irrespective of the particular form of the function $\zeta(E_i)$. Note that there is no combinatory involved in a such procedure. what remain in the sequence are the fluctuations away from unit mean. Next, one defines the spacing $s_i=x_{i+1}-x_i$ between two adjacent points. Collecting s_i in a histogram, one obtains the probability density or the nearest-neighbor spacing distribution (NND). In general, this procedure does not involve any uncertainty or spurious contributions and deals with a direct pro-

cessing of physical data. If the "events" $\{x_i\}$ are independent, i.e., correlations in the system under consideration are absent, the form of the histogram must follow $p(s)=\exp(-s)$, which is known as the Poisson density. The Poisson spectrum corresponds to the dominance of many crossings between different energies (momenta). On the other hand, if the levels are repelled, the density is approximately given by the Wigner surmise form

$$p(s)=\frac{\pi}{2}s\exp\left(-\frac{\pi}{4}s^2\right)$$

for the GOE. In turn, the crossings are usually observed when there is no mixing between states that are characterized by different good quantum numbers, while the anti crossings signal a strong mixing due to a perturbation brought about by either external or internal sources. In other words, any correlations that produce the deviation from the regular pattern (Poisson distribution) produce a collective state (resonance), or some structural changes in the system under consideration would be uniquely identified from the change in the histogram shape. In order to reveal structural changes in the momentum distribution, we determine the smooth part $\zeta(E)$ using a polynomial function of the fifth order to interpolate the exact staircase function (see also Eq. (1)):

$$\zeta(E)=\sum\nolimits_{k=0}^{5}a_kE^k, \tag{2}$$

where $E=|p|$ are the momentum values in the given event. We recall that momenta are ordered in ascending series. The parameters a_k were optimized with the aid of the program MINUIT. (MINUIT is a numerical minimization computer program originally written in the FORTRAN programming language by CERN staff physicist Fred James in the 1970s. This program searches for minima in a user-defined function with respect to one or more parameters using several different methods, as specified by the user). Next, we obtain new spectra $\{x_i\}$ by the unfolding procedure of the original spectrum $\{E_i\}$ through the mapping of $E\rightarrow x$ by means of the polynomial function (2) with the optimized coefficients

$$a_k: x_i=\zeta(E_i),\ i=1\cdots,N.$$

Having a set of variables $\{x_i\}$, one is able to determine the set of spacings $\{s_i\}$. Since all events are independent, we apply the same procedure for the other events and obtain the new independent sets of spacings $\{s_i\}$.

To identify correlations, we divided the set of spacings $\{s_i\}$ into three sets, in correspondence with three regions of the measured momenta: (a) 0.1 < $|p|$ <1.14 GeV/c (Region Ⅰ); b) 1.14 < $|p|$ <4.0 GeV/c (Region Ⅱ); and c) 4.0 < $|p|$ <7.5 GeV/c (Region Ⅲ) (see Fig. 1–4). The region boundaries were determined with the requirement that the shape of the spacing density $p(s)$ does not change in the region under consideration. There is no other procedure to define such regions without the method described above, which has proved to be useful in data processing for various systems during the RMT analysis [8, 24]. In the present paper we consider the nearest-neighbor spacing momentum distribution for all charged secondary particles, and the nearest-neighbor spacing momentum distribution for $N_{\rm ch}$ [10–22] from experimental data, and then compare them with the nearest-neighbor spacing momentum distribution for all charged secondary particles and the nearest-neighbor spacing momentum distribution for $N_{\rm ch}$ [10–24] from the Dubna Cascade Model to the see changes with the increasing number of charged particles.

5 Results and discussion

In Figs. 1 and 3 we can see the distributions of $p(s)$ functions for all charged particles in the three regions of momentum as a function of the number of charged particles in the experimental events and those produced with the aid of the DCM. This analysis shows that the correlations are absent in Region Ⅰ (the Poisson distribution), while one observes the onset of the strong correlations in Region Ⅲ. The experiment and the model results confirm the existance of some peaks in Region Ⅱ and their transformation to the Wigner distribution in Region Ⅲ. Evidently, the experiment and the model results demonstrate the manifestation of some non-trivial non-kinematic correlations for the secondary charged particles in Region Ⅱ and Ⅲ.

To see changes with the increasing number of charged particles $N_{\rm ch,}$ we divided the events into three groups: i) the events with $N_{\rm ch}$=10–14 secondary charged particles; ii) the events with $N_{\rm ch}$=15–19 secondary charged particles; and iii) the events with $N_{\rm ch}$=20–22 secondary charged particles ($N_{\rm ch}$=20–24 for the DCM; see Figs. 2 and 4). The separation was also done according to the criteria discussed above.

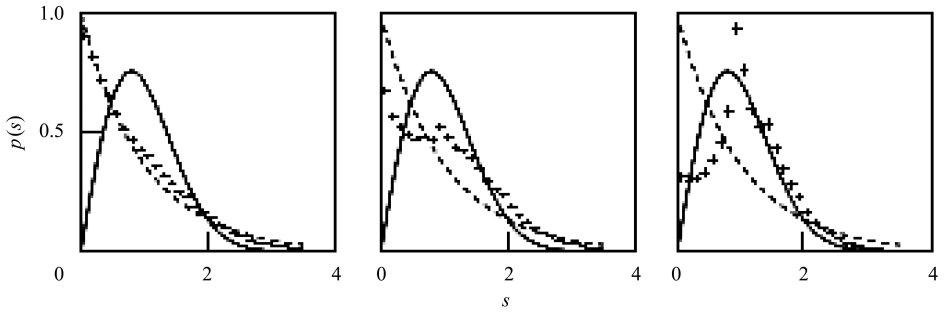

Fig. 1. The experimental data for all charged secondary particles, the nearest neighbor spacing momentum distribution (histogram) $p(s)$ for different regions of measured momenta: the left panel corresponds to $0.1< |p| <1.14$ GeV/c; the middle panel corresponds to $1.14< |p| <4.0$ GeV/c; and the right panel corresponds to $4.0< |p| <7.5$ GeV/c. The Poisson and the Wigner surmise distributions are connected by dashed and solid lines, respectively.

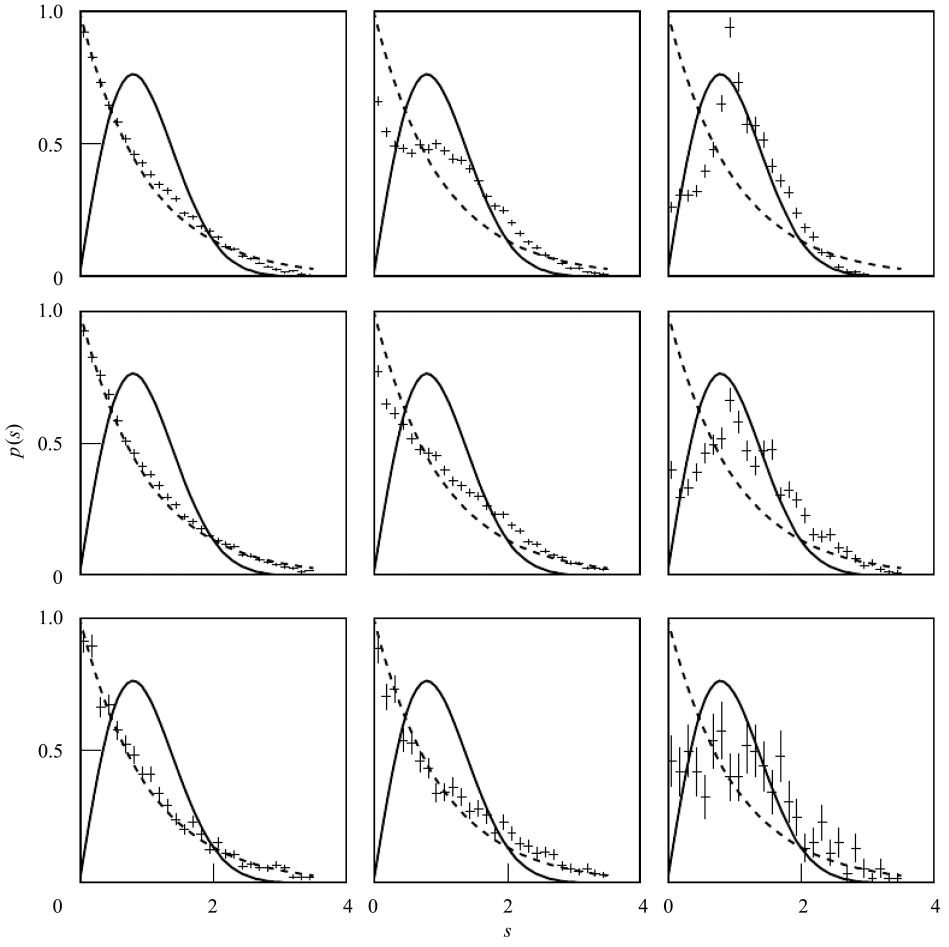

Fig. 2. The experimental data for all charged secondary particles; the nearest neighbor spacing momentum distribution (histogram) $p(s)$ for different regions of measured momenta: the first column corresponds to $0.1< |p| <1.14$ GeV/c; the second column corresponds to $1.14< |p| <4.0$ GeV/c; and the third column corresponds to $4.0< |p| <7.5$ GeV/c. The NND distribution for different multiplicities $N_{\rm ch}$: the top row corresponds to $N_{\rm ch}$=10–14; the middle row corresponds to $N_{\rm ch}$=15–19; and the bottom row corresponds to $N_{\rm ch}$=20–22. The Poisson and the Wigner surmise distributions are connected by dashed and solid lines, respectively.

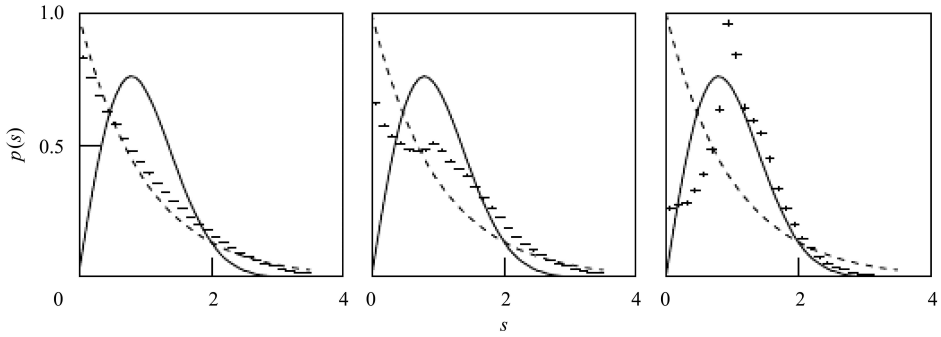

Fig. 3. The DCM data for all charged secondary particles; the nearest neighbor spacing momentum distribution (histogram) $p(s)$ for different regions of measured momenta: the left panel corresponds to $0.1< |p| <1.14$ GeV/c; the middle panel corresponds to $1.14< |p| <4.0$ GeV/c; and the right panel corresponds to $4.0< |p| <7.5$ GeV/c. The Poisson and the Wigner surmise distributions are connected by dashed and solid lines, respectively.

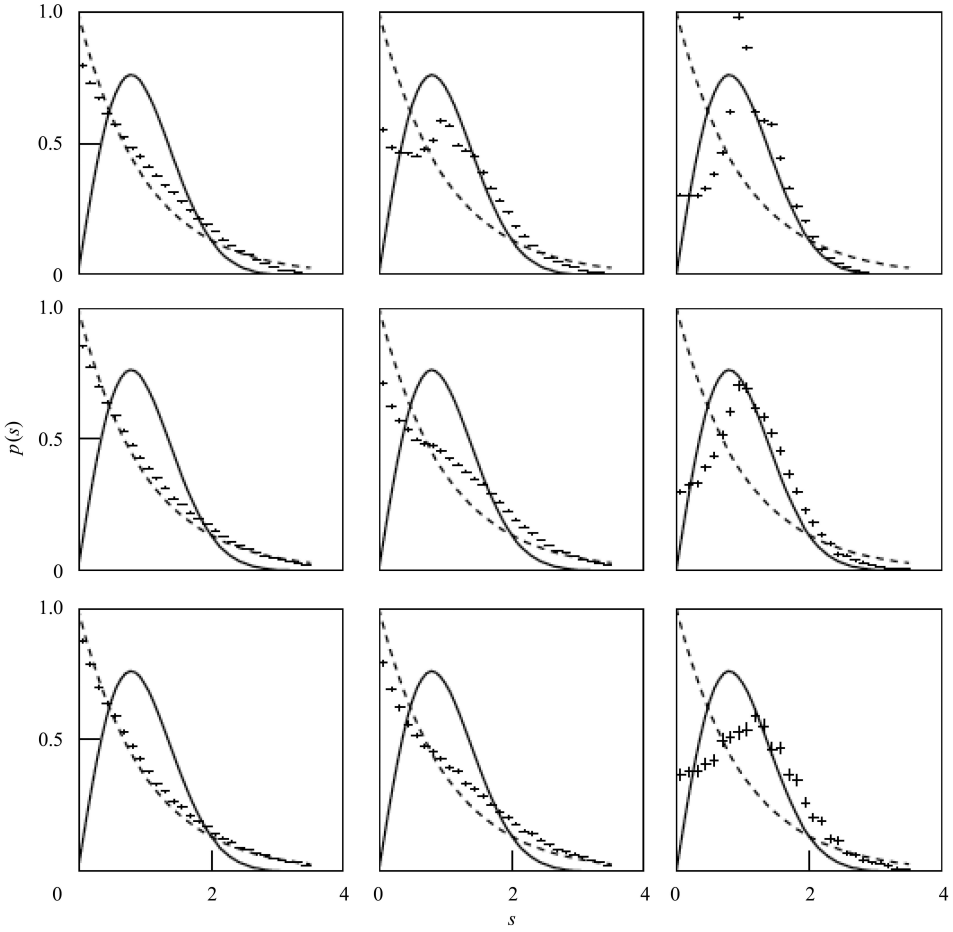

Fig. 4. The DCM data for all charged secondary particles; nearest neighbor spacing momentum distribution (histogram) $p(s)$ for different regions of measured momenta: the first column corresponds to $0.1< |p| <1.14$ GeV/c; the second column corresponds to $1.14< |p| <4.0$ GeV/c; and the third column corresponds to $4.0< |p| <7.5$ GeV/c. The NND distribution for different multiplicities $N_{\rm ch}$: the top row corresponds to $N_{\rm ch}$=10–14; the middle row corresponds to $N_{\rm ch}$=15–19; and the bottom row corresponds to $N_{\rm ch}$=20–24. The Poisson and the Wigner surmise distributions are connected by dashed and solid lines, respectively.

We have found that strong correlations are brought about by the proton pairs with zero angle in the momentum distribution interval 4.0< $|p|$ <7.5 GeV/c. This interpretation becomes even more convincing with the increase charged particles, as shown in the right column of Figs. 2 and 4. With the increase in the multiplicity of secondary charged particles, the number of stripping protons decreases. As a result, the correlations, brought by these proton pairs, decreases as well. For the multiplicity $N_{\rm ch}$=20–22 from the experiment and $N_{\rm ch}$=20–24 from the DCM, the distribution is neither the Poisson nor the Wigner surmise. Note, however, that the number of participants is increased, which can be associated with the onset of the central collisions.

The correlations are absent in Region I (the Poisson distribution), while one can observes the following:

1) The behavior of $p(s)$ functions from Regions II and III changes with the increasing number of charged particles.

2) The structure (deviation from the Poisson distribution) disappears in Region II with the increasing number of charged particles.

3) The Wigner tape behavior disappears (or become weaker, essentially) in Region III with increasing the number of charged particles.

4) So results from Figs. 2 and 4 demonstrate evidently that the observed structure for the $p(s)$ behavior in Regions II and III is related to the multiplicity. At high multiplicities we observe that the correlations (which lead to the deviation from the Poisson behaviour of the NND for $|p|$>1.15 GeV/c) essentially decrease.

6 Conclusion

In conclusion, using the procedure provided by the RMT approach, we found that the correlation decreases with the increasing number of charged particles $N_{\rm ch}$ produced by the nucleus-nucleus collisions, using the procedure based on the RMT approach. We stress that this procedure is based on the direct processing of the experimental data and the simulated data from the Dubna Cascade Model. The transition from the Poisson distribution to the Wigner surmise distribution signals on onset of correlations. In turn, the centrality of nucleus-nucleus collisions is associated with the absence of correlations.

References

1 Aichelin J, Werner K. Phys. Rev. C, 2009, **79**: 064907
2 BRAHMS collaboration, Arsene I C, J. Phys. G: Nucl. Part. Phys., 2009, **36**: 064004
3 PHENIX collaboration, Masui H. Eur. Phys. J. C, 2009, **62**: 169
4 Soltz R A, Newby R J, Klay J L, Heffner M, Beaulieu L, Lefort T, Kwiatkowski K, Viola V E. Phys. Rev. C, 2009, **79**: 034607
5 PHOBOS collaboration, Gburek T. J. Phys. G: Nucl. Part. Phys., 2008, **35**: 104131
6 STAR collaboration, Masui H. J. Phys. G: Nucl. Part. Phys., 2009, **36**: 064047
7 Shahaliev E I, Nazmitdinov R G, Kuznetsov A A, Syleimanov M K, Teryaev O V. Physics of Atomic Nuclei, 2006, **69**: 142
8 Brody T A, Flores J, French J B, Mello P A, Pandy A, Wong S S M. Rev. Mod. Phys., 1981, **53**: 385
9 Mehta M L. Random Matrices Elsevier, Amsterdam, Third Edition. 2004
10 Nazmitdinov R G, Shahaliev E I, Syleimanov M K, Tomsovic S. Phys. Rev. C, 2009, **79**: 054905
11 BBCDHSSTTU-BW collaboration, Balea O et al. Phys. Lett., B, 1972, **39**: 571
12 Akhababian N et al. JINR Report, No. 1-12114, Dubna 1979
13 BBCDHSSTTU-BW collaboration, Armutliiski D D et al. Yad. Fiz., 1987, **45**: 1047
14 Agakishiyev H N et al. Zeit. für Physik C-Particles and Fields, 1985, **27**: 177
15 Barashenkov V S, Toneev V D. Interaction of High Energy Particles and Atomic Nuclei with Nuclei. Moscow, Atomizadt, 1972
16 Gudima K K, Toneev V D. Physics Letters B, 1978, **73**: 293
17 Gudima K K, Iwe H, Toneev V D. Journal Physics G, 1979, **5**: 229
18 Gudima K K, Titov A I, Toneev V D. Physics Letters B, 1992, **287**: 302
19 Toneev V D, Gudima K K. Nuclear Physics A, 1983, **400**: 173c
20 Toneev V D, Gudima K K. Particle Production in Heavy-Ion Collisions at Intermediate Energies. GSI, Darmstadt, 1993. 52
21 Mashnik S G. In: Proceedings of a Specialists Meeting Intermediate Energy Nuclear Data: Models and Codes. Paris, 1994. 107
22 Blann M B, Gruppelaar H, Nagel P, Rodens J. International Code Comparison for Intermediate Energy Nuclear Data. NEA, OECD, Paris, 1994
23 Barashenkov V S, Zheregy F G, Musulmanbekov Zh.Zh. Preprint JINR P2-83-117, Dubna, 1983
24 Weidenmüller H A, Mitchell G E. Rev. Mod. Phys, 2009, **81**: 539